



(Received 1 April 2015; accepted 17 August 2016; first published online 1 September 2016)

Abstract

The degree of melting of the mantle beneath the South Atlantic Ocean has been estimated by modelling the evolution of the melt composition as it ascends through the mantle. The model uses a two-phase approach, in which the melt is considered to be a mixture of a melt phase and a residual solid phase. The model is constrained by the observed melt composition at the surface, and the degree of melting is determined by the depth at which the melt composition reaches a specific value. The model is able to predict the degree of melting for a range of melt compositions, and the results show that the degree of melting is generally low, typically less than 10% for most melt compositions. The model is also able to predict the degree of melting for a range of melt compositions, and the results show that the degree of melting is generally low, typically less than 10% for most melt compositions.

1. Introduction

The degree of melting of the mantle beneath the South Atlantic Ocean has been estimated by modelling the evolution of the melt composition as it ascends through the mantle. The model uses a two-phase approach, in which the melt is considered to be a mixture of a melt phase and a residual solid phase. The model is constrained by the observed melt composition at the surface, and the degree of melting is determined by the depth at which the melt composition reaches a specific value. The model is able to predict the degree of melting for a range of melt compositions, and the results show that the degree of melting is generally low, typically less than 10% for most melt compositions. The model is also able to predict the degree of melting for a range of melt compositions, and the results show that the degree of melting is generally low, typically less than 10% for most melt compositions.

The degree of melting of the mantle beneath the South Atlantic Ocean has been estimated by modelling the evolution of the melt composition as it ascends through the mantle. The model uses a two-phase approach, in which the melt is considered to be a mixture of a melt phase and a residual solid phase. The model is constrained by the observed melt composition at the surface, and the degree of melting is determined by the depth at which the melt composition reaches a specific value. The model is able to predict the degree of melting for a range of melt compositions, and the results show that the degree of melting is generally low, typically less than 10% for most melt compositions. The model is also able to predict the degree of melting for a range of melt compositions, and the results show that the degree of melting is generally low, typically less than 10% for most melt compositions.

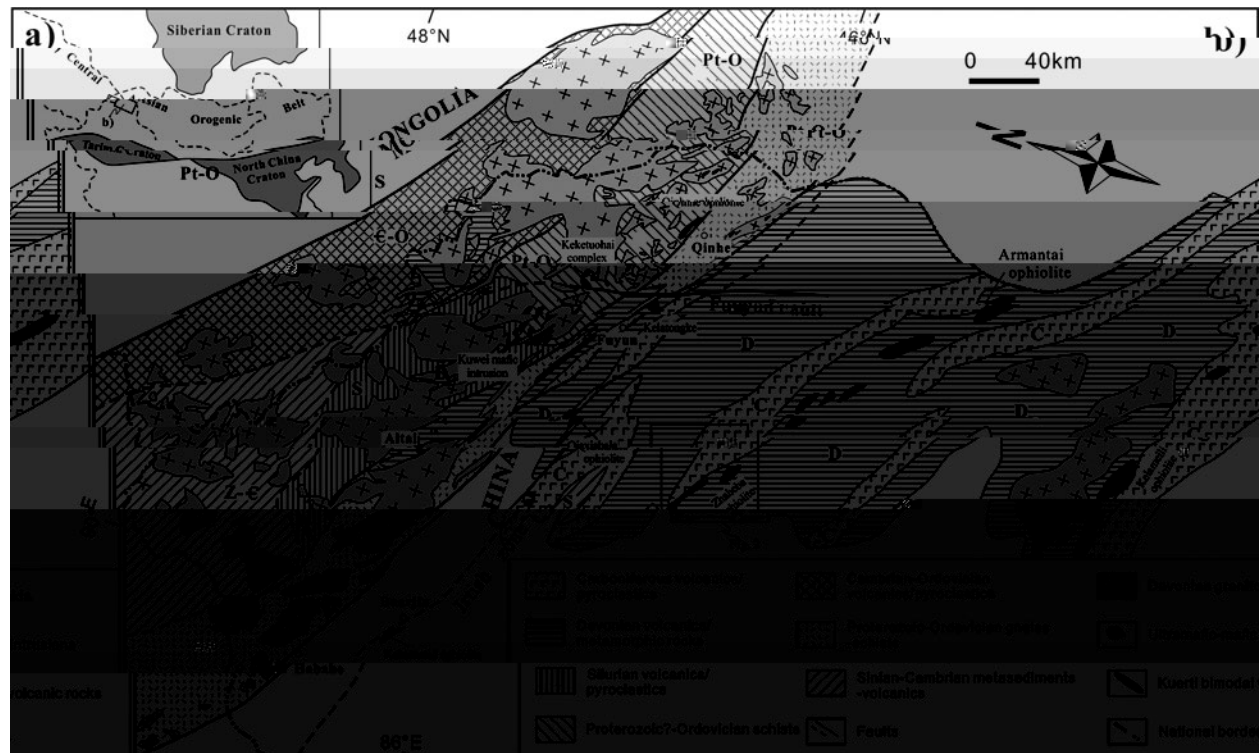
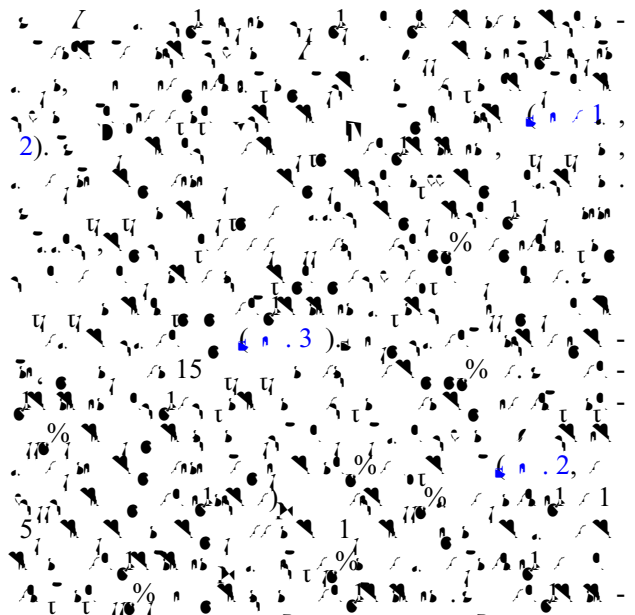
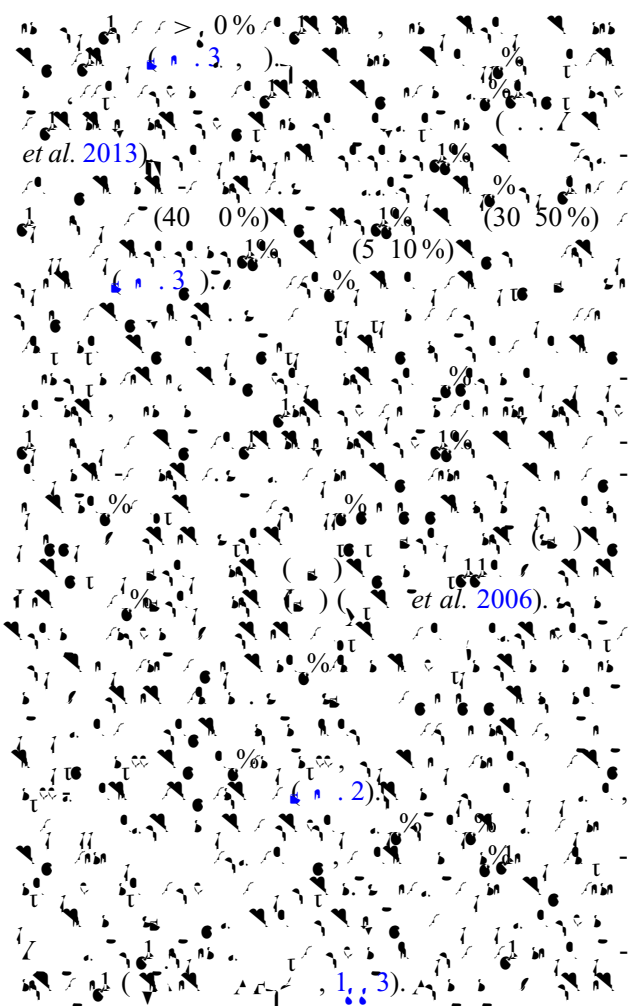


Fig. 1. (a) Regional geological sketch of the Pt-O orogeny belt (modified after Li *et al.* 2005).



2. Regional geology, field observations and petrography



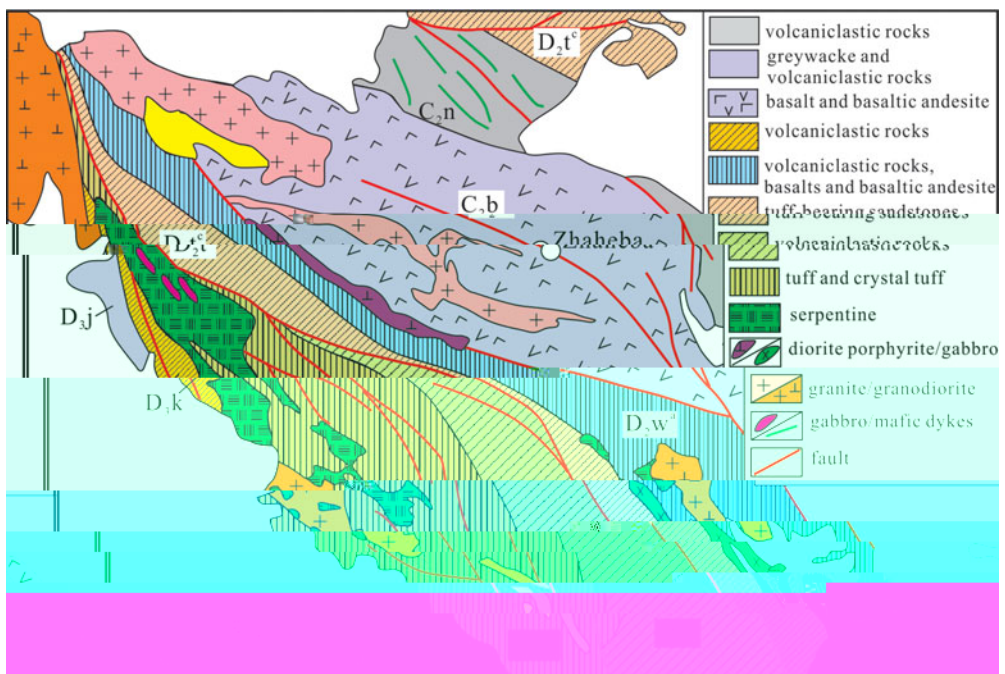


Fig. 2. Geological cross-section of the Zhaheba ophiolite. The cross-section shows the typical sequence of the ophiolitic structures (modified after Li et al. 2006; Wang et al. 2006). The main structures are D₂ (green), D₃ (red) and D₄ (blue).

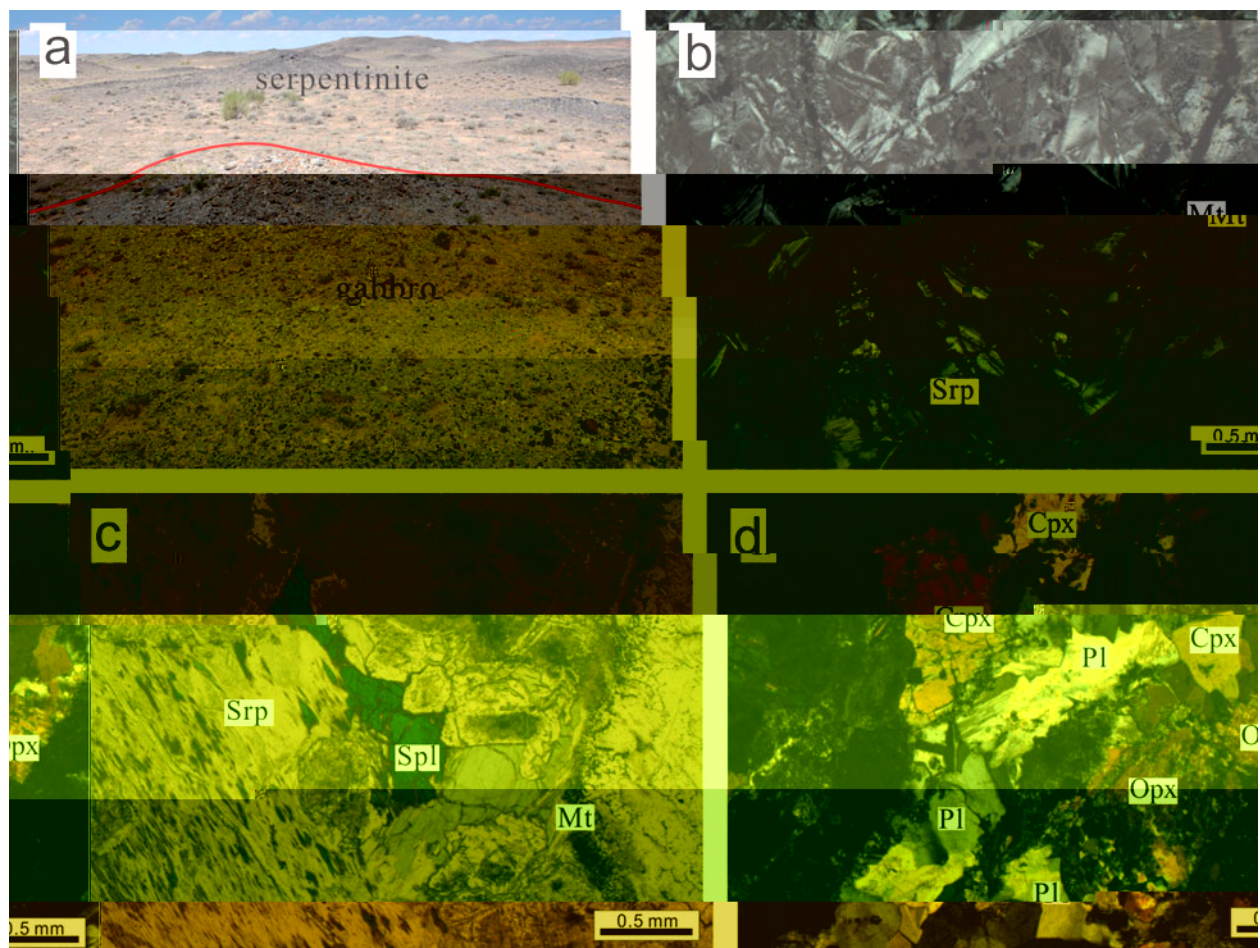


Fig. 3. (a) Serpentinite outcrop at the Zhaheba ophiolite. (b) Photomicrograph showing intergrowths of olivine and pyroxene in a gabbro sample. (c) Photomicrograph showing intergrowths of spinel and pyroxene in a gabbro sample. (d) Photomicrograph showing intergrowths of plagioclase, clinopyroxene, orthopyroxene and olivine in a gabbro sample. (e) Photomicrograph showing intergrowths of spinel and pyroxene in a gabbro sample. (f) Photomicrograph showing intergrowths of plagioclase, clinopyroxene, orthopyroxene and olivine in a gabbro sample.

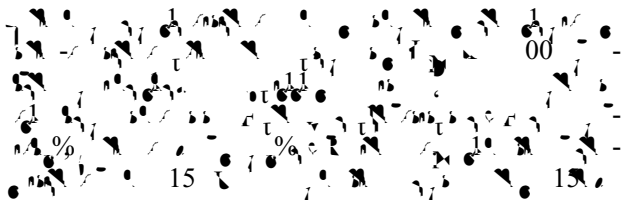


3. Analytical procedures

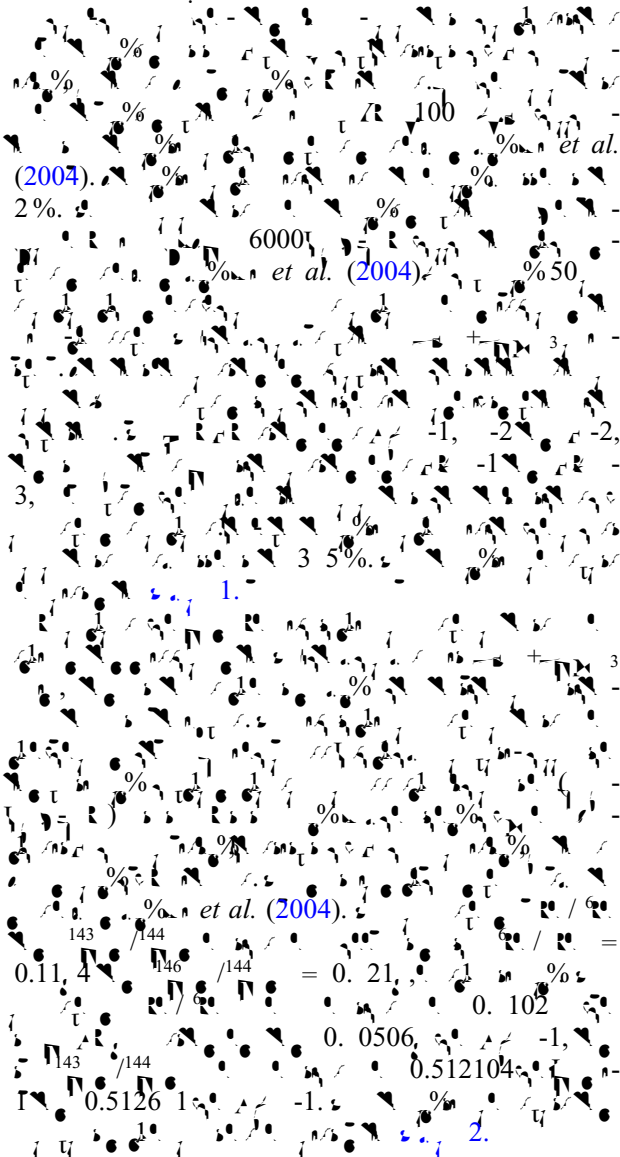
3.a. Zircon U-Pb dating and Hf-O isotope analyses

Zircon U-Pb dating and Hf-O isotope analyses were performed on two zircon fractions (2013-01, 46°32'51"S, 24°24'10"E; 2013-02, 46°33'22"S, 24°23'36"E) collected from the same sample (Fig. 1). The samples were previously analysed by *et al.* (2011), *et al.* (2010) and *et al.* (2003). The zircon fractions were separated from the host rock by hand-picking under a binocular microscope. The zircon grains are euhedral to subhedral, colourless to light brown, and range in size from 100 to 150 µm. The U-Pb ages were determined by the multi-collector ICP-MS method (Liu *et al.*, 2013). The analytical precision was ±0.21% (2σ) for the 2013-01 sample and ±0.2% for the 2013-02 sample. The Hf-O isotope analyses were performed using the laser ablation ICP-MS method (Liu *et al.*, 2010a). The analytical precision was ±0.21% (2σ) for the 2013-01 sample and ±0.2% for the 2013-02 sample. The δ¹⁸O values are expressed relative to PDB, and the error bars represent 1σ. The U-Pb ages and Hf-O isotope data are shown in Table 1.

3.b. Mineral analyses

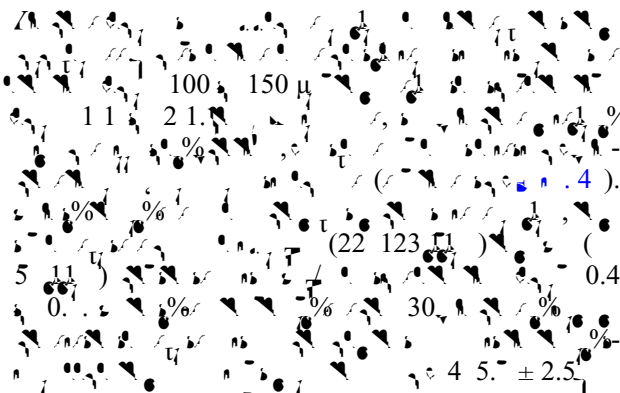


3.c. Whole-rock analyses



4. Analytical results

4.a. Zircon U-Pb ages



	2013-01-1	2013-01-3	2013-01-4	2013-01-5	2013-01-6	2013-01-	2013-01-	2013-01-1	2013-01-2	2013-01-4
Major elements (%)										
SiO ₂	3.0	4.20	3.41	3.62	3.22	3.2	3.05	4.22	46.4	51.2
Al ₂ O ₃	0.05	0.20	0.05	0.05	0.04	0.05	0.04	0.14	0.12	0.2
FeO	0.61	1.6	1.04	0.6	0.0	0.4	0.0	1.2	1.64	1.33
MnO	.44	4.6	.	.36	.5	.16	.4	3.6	3.24	3.
TiO ₂	0.0	0.10	0.11	0.11	0.11	0.0	0.11	0.0	0.0	0.0
CaO	3.21	24.5	3.2	3.4	3.0	3.31	3.44	10.04	4.03	5.4

Table 1.

	2013 Δ 01-1	2013 Δ 01-3	2013 Δ 01-4	2013 Δ 01-5	2013 Δ 01-6	2013 Δ 01-	2013 Δ 01-	2013 Δ 01-1	2013 Δ 01-2	2013 Δ 01-4
	2013 Δ 01-5	2013 Δ 01-6	2013 Δ 01- A (c 1)	2013 Δ 01- A (c 1)	2013 Δ 01- A (c 1)	2013 Δ 03-2 A (c 1)	2013 Δ 03-3 A (c 1)	2013 Δ 03-4 A (c 1)	2013 Δ 03-5 A (c 1)	2013 Δ 01-3 A (c 2)
<i>Major elements (%)</i>										
Si	4.1	45.	4 ..	53.1	51.1	50.40	50.54	50.52	51.22	52.3
Al	0.34	0.15	1.40	1.24	1.31	1.0	1.63	1.31	1.1	0.33
Mg	1.5	1.5	16.5	16.1	15.3	15.	16.6	15.55	15.4	1.61
Ca	4.52	3.34	3.44
Na	0.0	0.0	0.11	0.10	0.11	0.13	0.11	0.14	0.12	0.0
K	6.	.42	4.0	4.2	4.41	5.	3.2	6.06	.14	4.
Ti	11.03	12.61	6.22	5.5	6.3	6.5	4.52	4.	.26	..0
V	4.6	.3	.2	.3	.00	4.52	.31	4.0	4.0	.11
Cr	0.13	0.11	0.3	0.31	0.42	2.04	0.33	1.2	2.03	0.1
Mn	0.04	0.02	0.62	0.62	0.65	0.4	0.6	0.4	0.44	0.04
Fe	3.2	3.26	4.24	2.54	2.3	2.2	5.14	2.65	1.3	2.
Co	..5	..2	..6	..0	..4	..40	..1	..6	..6	..1
Ni	..5	..4	..11	..0	..42	..56	..64	..6	..11	..2
P	..5	..1	..55	..54	..54	..56	..41	..56	..64	..4
<i>Trace elements (ppm)</i>										
As	0	4.5	1.16	1.12	1.4	.0	40.4	5.2	6.2	5.1
Se	0.22	0.135	1.24	1.63	1.316	1.53	1.034	1.100	0.55	0.62
Br	25.0	23.	1.6	1.5	1.5	1.2	25.2	1.	1.	0
Li	11	3.	1.6	166	1.2	22	22	254	1	5.
Rb	34.	163	60.5	62.6	64.1	116	1.	0.	203	23.
Ba	24.2	21.6	26.	23.6	24.6	2.	2.5	2.0	2.0	16.4
La	4.	1.5	63.6	50.	51.4	6.	2.	5.3	132	1.1

Sample	Location	Depth (km)	Age (Ma)
2013-01-5	2013-01-5	3.24	3.24
2013-01-6	2013-01-6	1.20	1.20
2013-01-1	2013-01-1	3.60	3.60
2013-01-2	2013-01-2	46.0	46.0
2013-01-3	2013-01-3	43.30	43.30
2013-03-2	2013-03-2	23.40	23.40
2013-03-3	2013-03-3	43.00	43.00
2013-03-4	2013-03-4	25.20	25.20
2013-03-5	2013-03-5	32.0	32.0
2013-01-3	2013-01-3	6.56	6.56

Table 1.

	2013-01-11 (<i>n</i>)	2013-02-1 (<i>n</i>)	2013-02-2 (<i>n</i>)	2013-03-1 (<i>n</i>)	2013-03-6 (<i>n</i>)	2013-01-10 (<i>n</i>)	04/06 (<i>n</i>)	04/24 (<i>n</i>)	04/26 (<i>n</i>)	03/11 (<i>n</i>)
Trace elements (ppm)										
Si	1.4	36.4	42.4	26.0	32.4	1.7	/	/	/	/
Al	0.35	0.153	0.35	1.1	0.4	0.46	/	/	/	/
Mg	32.5	33.2	34.5	25.1	26.3	32.1	13.4	20.5	1.1	20.3
Ca	1.4	203	21	33	341	1.5	144	14	214	265
Na	56.5	44.2	4	1	22.2	53	15	162	214	265
K	34.	3.5	3.3	23.1	24.	33.	20.6	30.	2.	20.2
Sc	66.4	4.6	6.4	25.4	2.1	66.6	1.1	114	5.5	.02
Ti	6.4	236.4	256.	205.4	20	114.20	/	/	/	/
V	4.0	44.1	4.0	4.	103	44.1	/	/	/	/
Cr	12.0	11.1	11.2	14.	13.6	12.0	/	/	/	/
Mn	0.5	1.420	1.00	3.130	3.20	0.53	4.	1.1	22.0	1.2
Fe	1.50	5.	20	24	66	1	31	111	11	6
Co	13.0	13.0	13.2	21.1	22.	12.5	13.2	13.2	14.	20.1
Ni	54.	42.3	41.5	144	154	52.	243	133	164	151
Cu	1.2	0.4	0.55	11.315	11.5	1.25	20.2	12.	21.	12.2
Zn	0.025	0.030	0.02	0.051	0.052	0.02	/	/	/	/
Pb	0.31	0.26	0.32	1.560	1.450	0.360	/	/	/	/
Hg	0.2	1.20	1.030	0.365	0.406	0.336	/	/	/	/
As	11	32	346	25	50	4.3	/	/	/	/
S	10.0	.40	.610	26.40	26.0	10.50	30.6	32.2	40.1	26.4
Cl	23.00	1.0	1.40	51.50	54.0	22.30	5.	62.	2.3	52.5
B	2.0	2.520	2.510	5.50	6.10	2.60	6.	4	10.5	6.4
Li	11.0	11.0	11.60	22.30	24.30	11.60	2.5	31.2	43.1	24.4
Be	2.540	2.00	2.60	4.40	4.00	2.30	4.5	5.2	6.	4.5
Rb	0.6	0.1	0.0	1.163	1.25	0.3	1.45	1.5	2.0	1.03
Y	2.40	2.13	2.54	4.14	4.46	2.522	3.56	4.01	5.35	4.23
La	0.36	0.3	0.3	0.612	0.660	0.34	0.4	0.54	0.64	0.63
Eu	2.10	2.150	2.220	3.420	3.60	2.130	2.5	2.	3.24	3.5
Gd	0.46	0.446	0.444	0.2	0.5	0.46	0.4	0.52	0.5	0.
Tb	1.350	1.230	1.240	2.120	2.20	1.310	1.32	1.3	1.45	2.25
Dy	0.10	0.16	0.15	0.304	0.32	0.14	0.1	0.2	0.2	0.34
Er	1.210	1.050	1.120	1.60	2.110	1.210	1.25	1.23	1.24	2.13
Tm	0.14	0.164	0.165	0.21	0.323	0.13	0.20	0.1	0.1	0.34
Lu	1.30	0.41	1.040	3.20	3.510	1.460	5.3	3.2	4.16	3.2
Yb	0.04	0.062	0.051	0.5	0.644	0.0	1.35	0.6	1.16	0.6
Ta	0.151	2.0	1.50	2.5	1.	0.33	/	/	/	/
W	0.34	0.206	0.200	45.20	35.10	0.41	.13	.0	4.1	21.06
Os	1.0	0.61	0.1	.60	.20	1.0	4.50	2.63	3.20	.41
Pt	0.500	0.304	0.302	2.30	3.40	0.501	1.	0.6	1.46	2.5.

04/06, 04/26, 04/2, 04/1, et al. (200, a).

	U_{f}	U_{d}	$(\text{U}_{\text{f}}/\text{U}_{\text{d}})_{\text{N}}$	$(\text{U}_{\text{f}}/\text{U}_{\text{d}})_{\text{N}} / (\text{U}_{\text{f}}/\text{U}_{\text{d}})_{\text{N}(\sigma)}$	$(\text{Pb}_{\text{f}}/\text{Pb}_{\text{d}})_{\text{N}}$	$(\text{Pb}_{\text{f}}/\text{Pb}_{\text{d}})_{\text{N}} / (\text{Pb}_{\text{f}}/\text{Pb}_{\text{d}})_{\text{N}(\sigma)}$						
2013-01-3	0.36	3.2	0.002	0.04030(2)	0.04015	2.4	10.	0.13, 4	0.512, 3, (40)	0.5124, 4	6.	
2013-01-10	0.5	6.6	0.0024	0.04, 5, (23)	0.04, 45	2.3	11.6	0.1235	0.512, 0, (43)	0.5124, 6	1.	
2013-03-1	3.13	2.0	0.0335	0.06324(20)	0.06133	4.4	22.3	0.121	0.512533(4)	0.512214	1.	
2013-03-2	2.	1320	0.0063	0.042, (20)	0.04255	4.5	2.6	0.1046	0.512, 1, (51)	0.512445	6.3	
2013-03-3	.06	516	0.0452	0.0536, (43)	0.05111	5.	36.	0.0,	0.512, 0, (30)	0.512450	6.4	
2013-03-4	.65	14.0	0.01	0.0422, (51)	0.04120	4.55	24.5	0.1123	0.512, 03(53)	0.51250,	.5	

$$\varepsilon_{\text{Pb}}(t) = 10000 \left(\frac{^{206}\text{Pb}}{^{238}\text{U}} \right) \lambda(t) / (^{143}\text{Nd} / ^{144}\text{Nd}) - \tau^{\star}(t) - 1 \quad \varepsilon_{\text{Pb}}(t) = \left(\frac{^{206}\text{Pb}}{^{238}\text{U}} \right) \text{MSWD} = 3.1 \quad N = 27$$

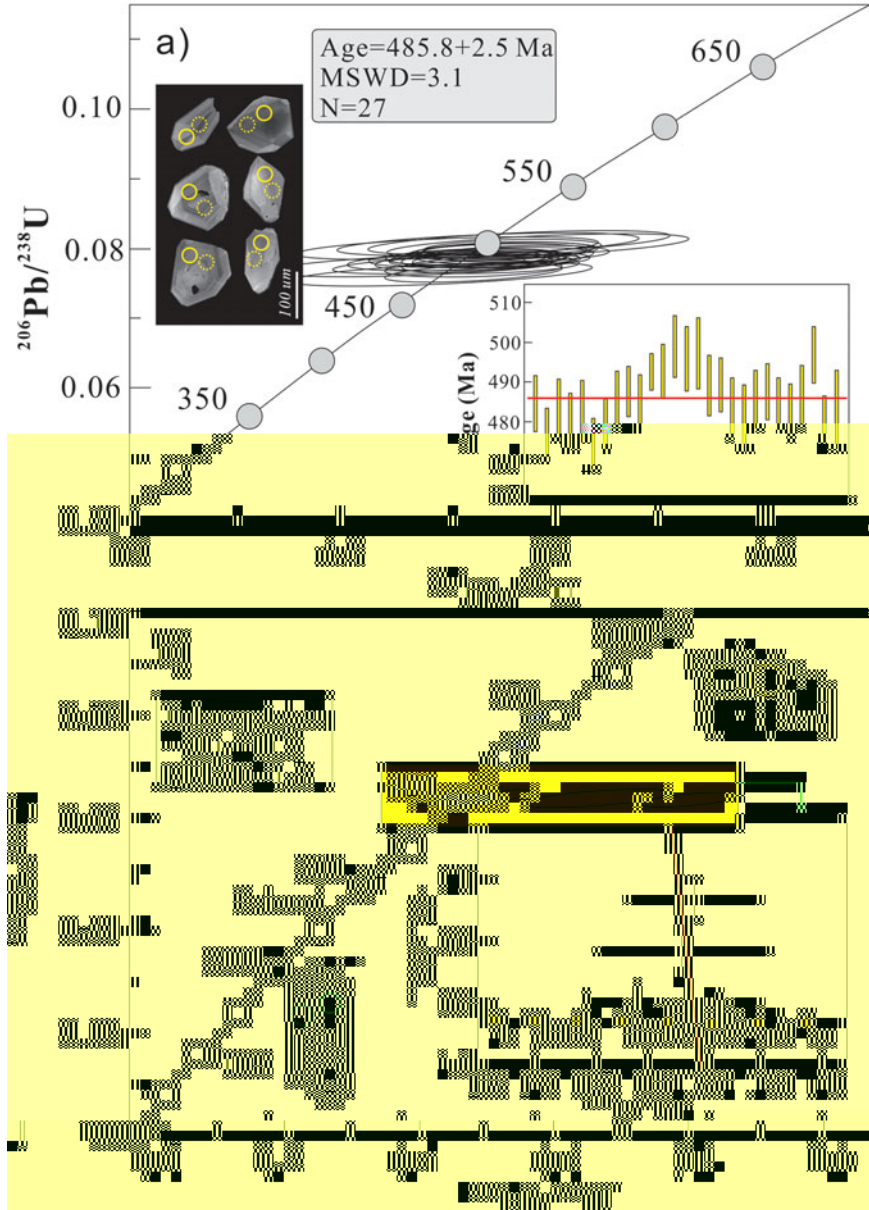
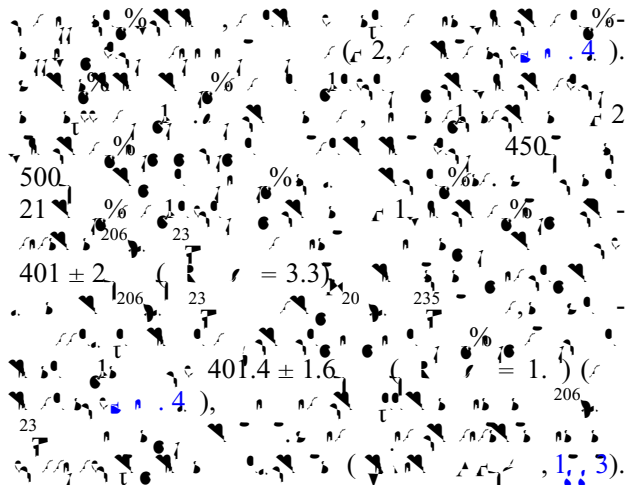


Fig. 4. (a) Concordia diagram of the $^{206}\text{Pb}/^{238}\text{U}$ vs. $^{143}\text{Nd}/^{144}\text{Nd}$ ratio for the Zhaheba ophiolite. The data points are labeled with their respective ages. The inset shows a micrograph of zircon grains with yellow circles indicating the locations of the analyzed spots. (b) Multi-stage Pb loss model for the Zhaheba ophiolite.

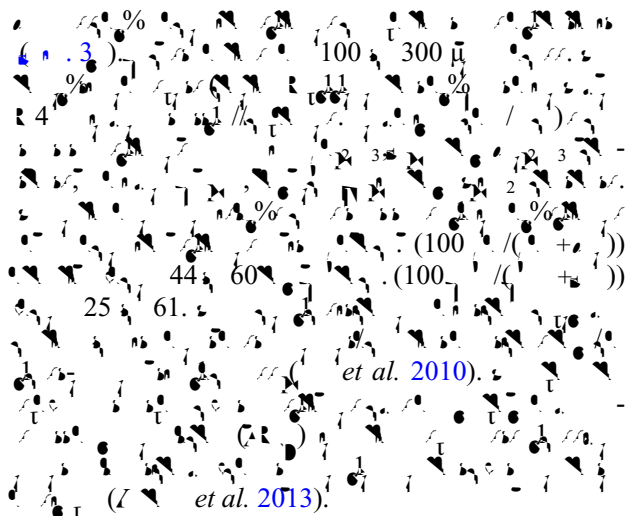
Fig. 4. $\text{MSWD} = 2$, $\text{N} = 3.1$, $\varepsilon_{\text{Pb}} = 3.1$, $\varepsilon_{\text{Nd}} = 4 \pm 4$, $\tau^{\star} = 100 \pm 40 \text{ Ma}$ ($\text{N} = 27$) (Zhang *et al.* 2003).

Fig. 4. $\text{MSWD} = 1.3$, $\text{N} = 0.0$, $\varepsilon_{\text{Pb}} = 1.3$, $\varepsilon_{\text{Nd}} = 0 \pm 0$, $\tau^{\star} = 100 \pm 40 \text{ Ma}$ ($\text{N} = 27$) (Zhang *et al.* 2003).

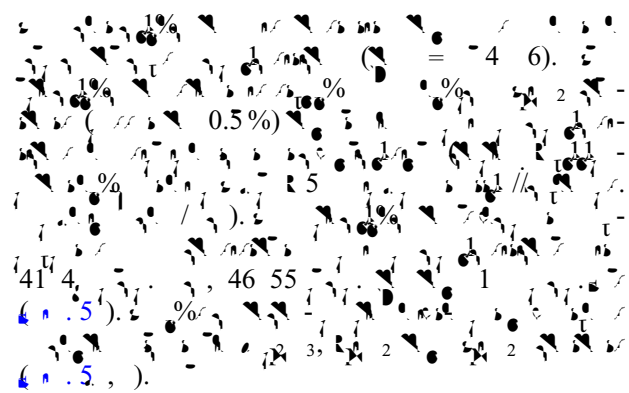


4.b. Mineral compositions

4.b.1. Spinel composition

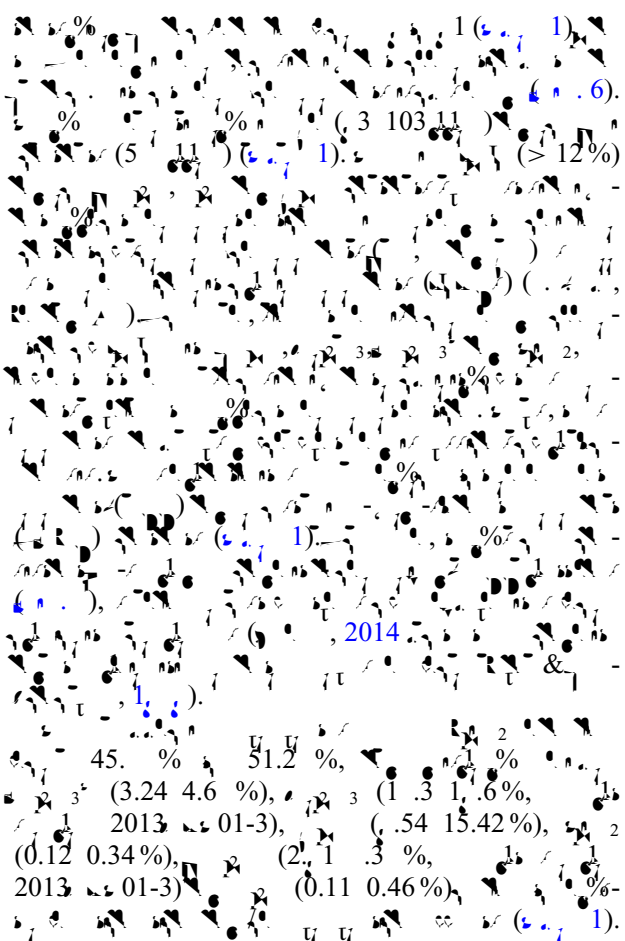
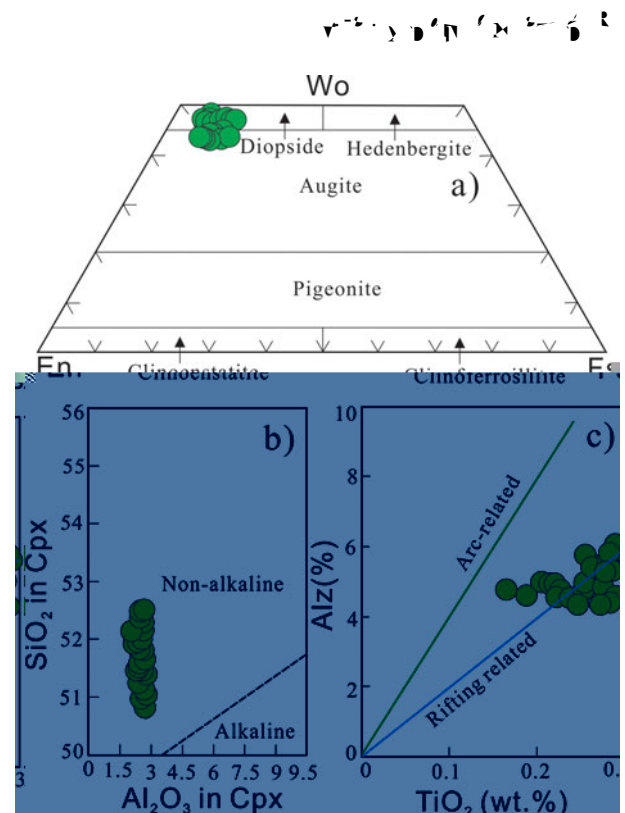
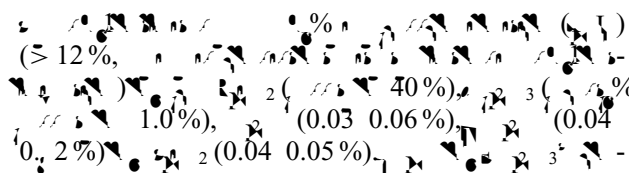


4.b.2. Pyroxene compositions



4.c. Whole-rock elemental geochemistry

4.c.1. Serpentinites and cumulates



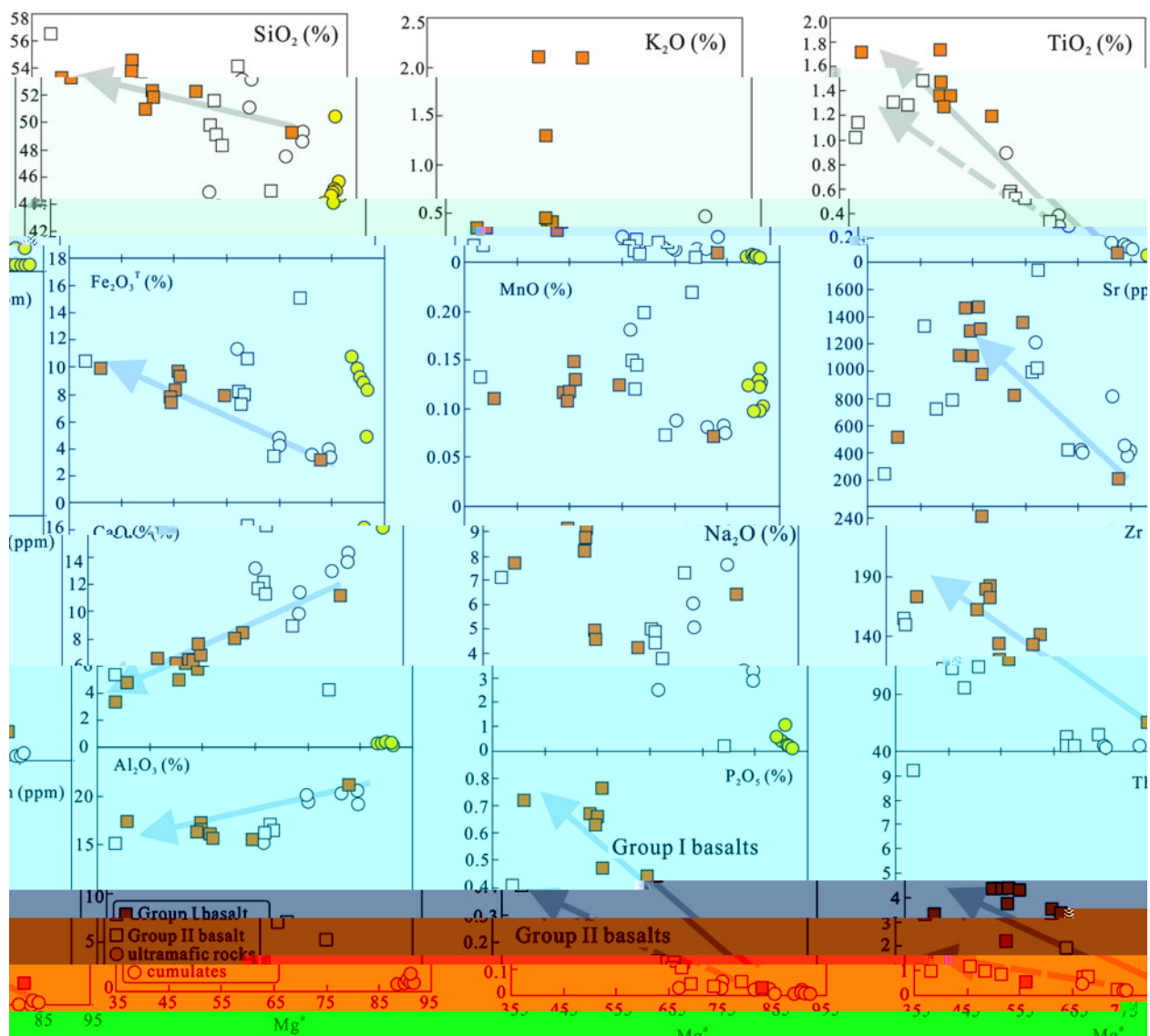
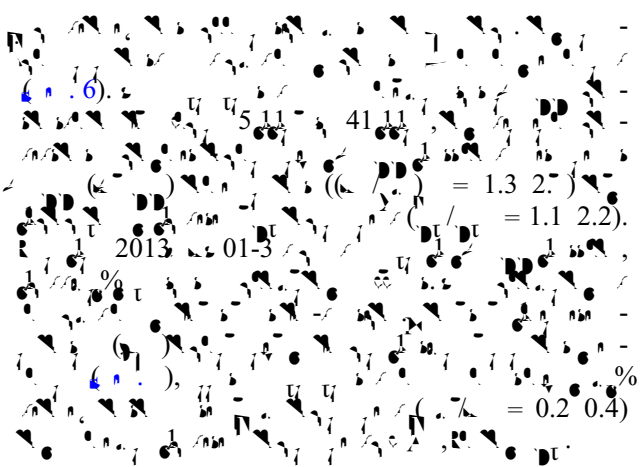
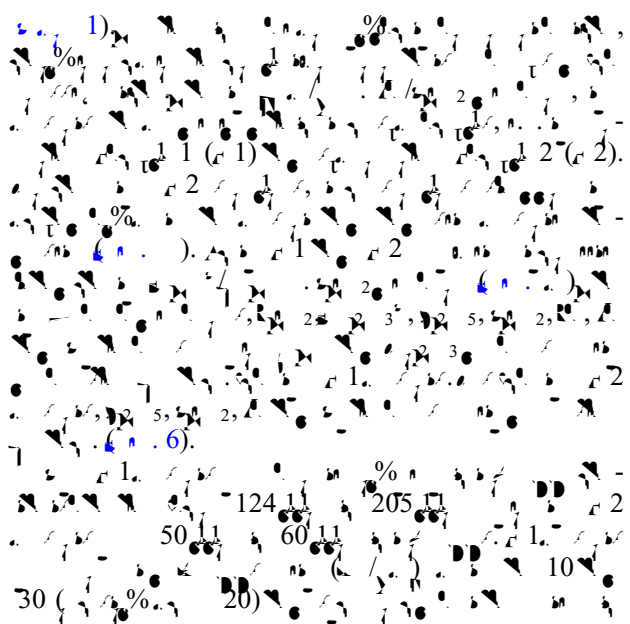


Fig. 6. (a) Major element plots showing the variation of major elements (wt%) versus Mg# for Group I and Group II basalts, and ultramafic rocks. Arrows indicate the trend from ultramafic rocks towards basalts. The legend indicates the symbol for each sample type: Group I basalt (orange square), Group II basalt (white square), and ultramafic rocks (open circle). The bottom panel shows the variation of Mg# versus Mg#.



4.c.2. Basalts

The basalts show a wide range of Mg# (35–95), with 43.15% having 35–45%, 5.65% having 45–55%, 52% having 55–65%, and 30% having 65–95%.



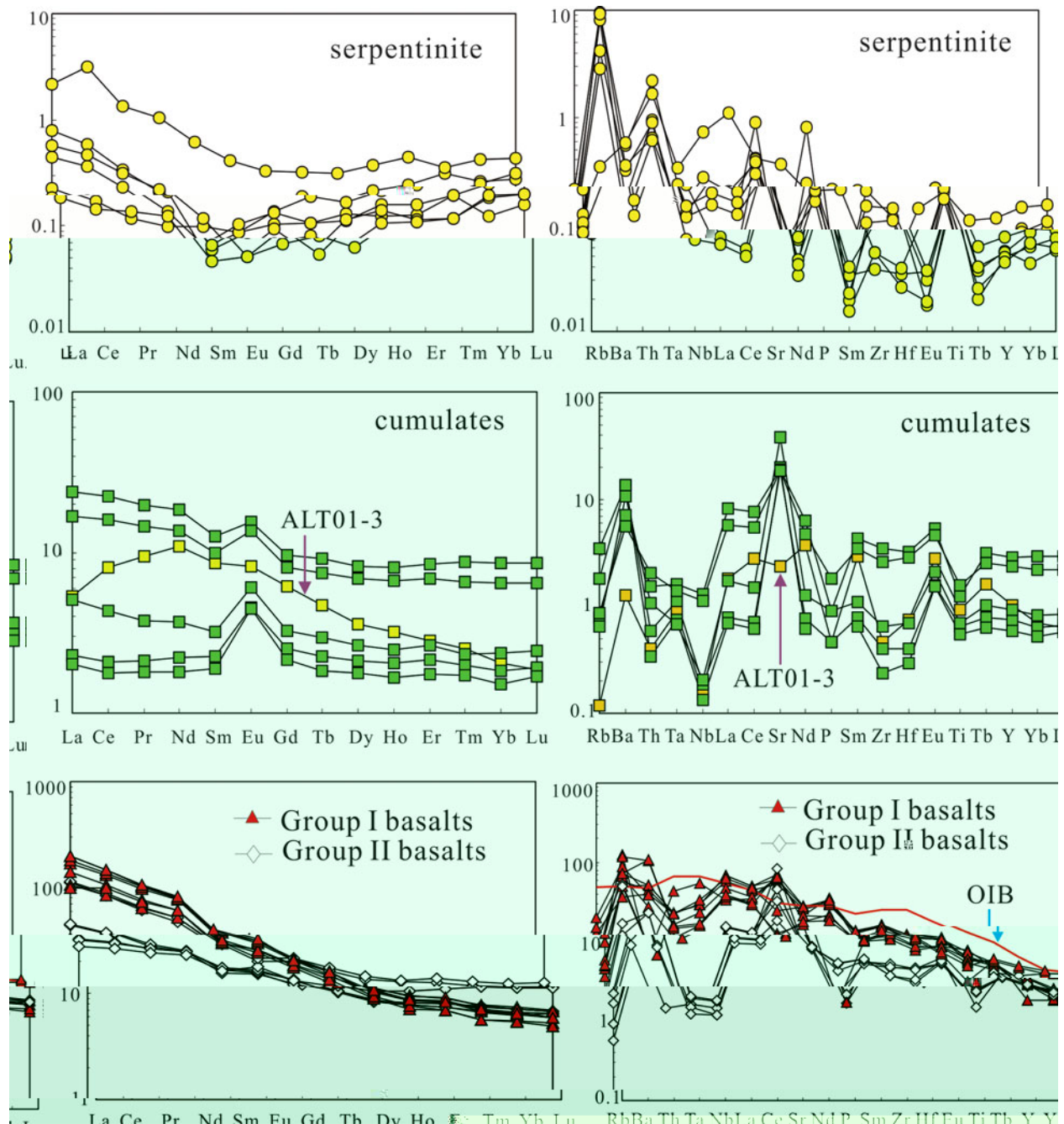


Fig. 1. REE patterns of the serpentinite and cumulates, and REE patterns of basalts from Group I and Group II. The pink shaded field indicates REE enrichment, and the green shaded field indicates REE depletion.

the REE patterns of the basalts from Group I and Group II are similar, with the REE patterns of the basalts from Group I being enriched in La and Ce, and depleted in Lu, while the basalts from Group II are enriched in La, Ce, Nd, Sm, Eu, Gd, Tb, Dy, Ho, Er, Tm, Yb, Lu, and depleted in Rb, Ba, Th, Ta, Nb, Sr, Nd, P, Sm, Zr, Hf, Eu, Ti, Tb, Y, Yb, and Lu (Fig. 1). The REE patterns of the basalts from Group I and Group II are similar to those of the Ocean Island Basalt (OIB) (Fig. 1).

4. Whole-rock Sr-Nd and Hf-O isotopes

The whole-rock Sr-Nd and Hf-O isotopes of the basalts from Group I and Group II are shown in Fig. 2. The Sr-Nd and Hf-O isotopes of the basalts from Group I and Group II are similar, with the Sr-Nd and Hf-O isotopes of the basalts from Group I being enriched in Sr, Nd, and Hf, and depleted in O, and the Sr-Nd and Hf-O isotopes of the basalts from Group II being enriched in Sr, Nd, and Hf, and depleted in O (Fig. 2).

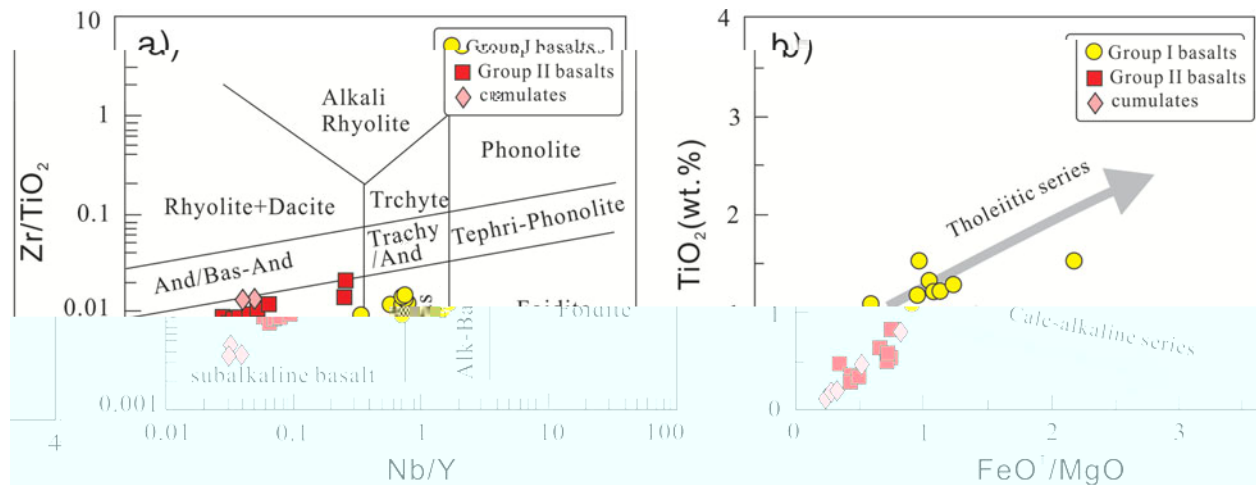


Fig. 2. (a) Zr/TiO_2 vs. Nb/Y ; (b) TiO_2 (wt. %) vs. FeO^+/MgO . The arrows indicate the differentiation trends of the basalts. The symbols represent Group I basalts (yellow circles), Group II basalts (red squares) and cumulates (pink diamonds).

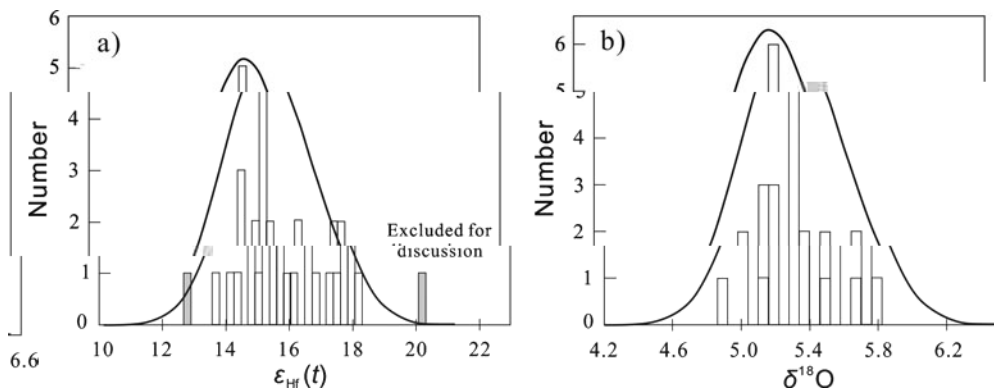


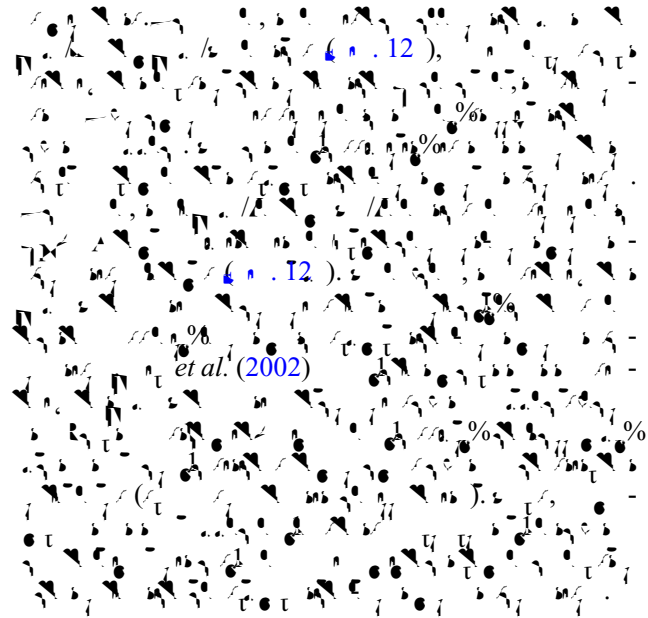
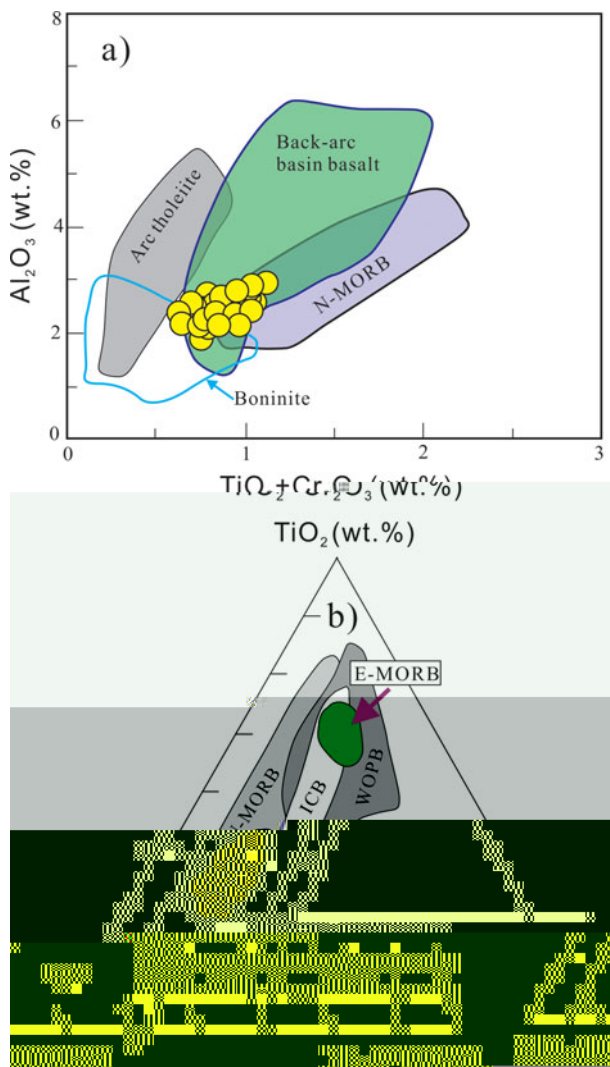
Fig. 3. Histograms showing the distribution of (a) $\epsilon_{Hf}(t)$ and (b) $\delta^{18}O$ values.

$\epsilon_{Hf}(t)$ (2013 = 01) (%)
 11.5 (4.5%), 12.5 (5.5%), 13.5 (20.2%), 14.5 (1.5%), 15.5 (4.1%), 16.5 (5.3%), 17.5 (1.1%), 18.5 (5.3%)
 $\delta^{18}O$ (~400) (‰)
 20.1 (1.4%), 21.0 (6.0%), 22.0 (1.2%), 23.0 (1.1%), 24.0 (1.1%), 25.0 (1.1%), 26.0 (1.1%), 27.0 (1.1%), 28.0 (1.1%), 29.0 (1.1%), 30.0 (1.1%), 31.0 (1.1%), 32.0 (1.1%), 33.0 (1.1%), 34.0 (1.1%), 35.0 (1.1%), 36.0 (1.1%), 37.0 (1.1%), 38.0 (1.1%), 39.0 (1.1%), 40.0 (1.1%), 41.0 (1.1%), 42.0 (1.1%), 43.0 (1.1%), 44.0 (1.1%), 45.0 (1.1%), 46.0 (1.1%), 47.0 (1.1%), 48.0 (1.1%), 49.0 (1.1%), 50.0 (1.1%), 51.0 (1.1%), 52.0 (1.1%), 53.0 (1.1%), 54.0 (1.1%), 55.0 (1.1%), 56.0 (1.1%), 57.0 (1.1%), 58.0 (1.1%), 59.0 (1.1%), 60.0 (1.1%), 61.0 (1.1%), 62.0 (1.1%), 63.0 (1.1%), 64.0 (1.1%), 65.0 (1.1%), 66.0 (1.1%), 67.0 (1.1%), 68.0 (1.1%), 69.0 (1.1%), 70.0 (1.1%), 71.0 (1.1%), 72.0 (1.1%), 73.0 (1.1%), 74.0 (1.1%), 75.0 (1.1%), 76.0 (1.1%), 77.0 (1.1%), 78.0 (1.1%), 79.0 (1.1%), 80.0 (1.1%), 81.0 (1.1%), 82.0 (1.1%), 83.0 (1.1%), 84.0 (1.1%), 85.0 (1.1%), 86.0 (1.1%), 87.0 (1.1%), 88.0 (1.1%), 89.0 (1.1%), 90.0 (1.1%), 91.0 (1.1%), 92.0 (1.1%), 93.0 (1.1%), 94.0 (1.1%), 95.0 (1.1%), 96.0 (1.1%), 97.0 (1.1%), 98.0 (1.1%), 99.0 (1.1%), 100.0 (1.1%).

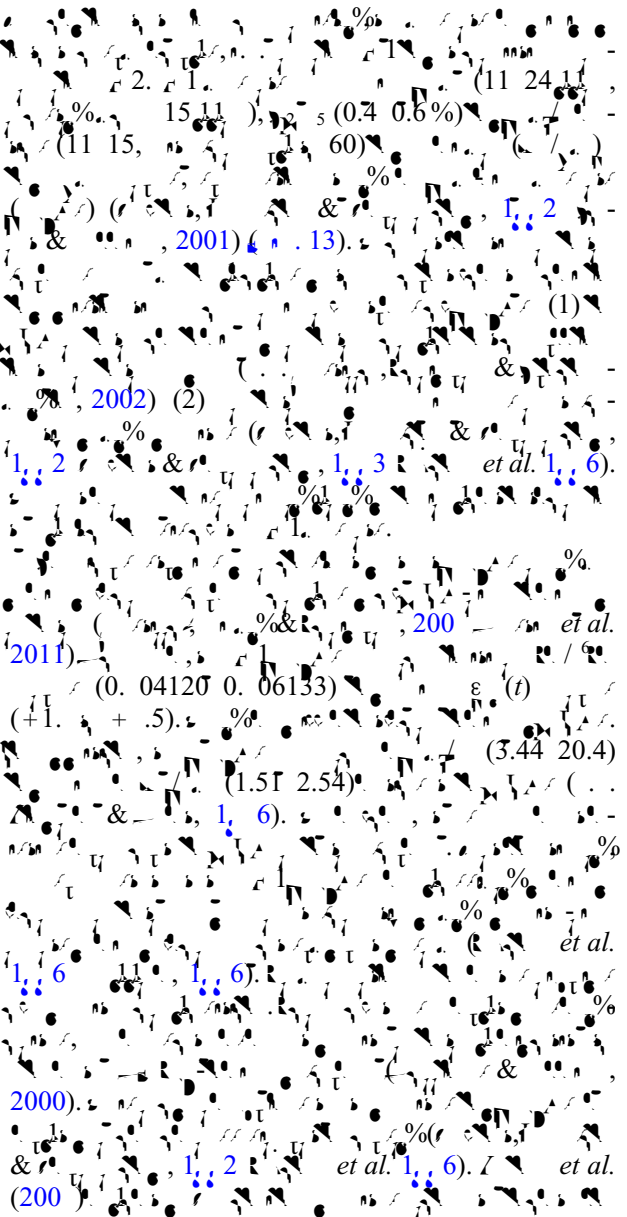
5. Discussion

5.a. The individual members of the Zhaheba ophiolite

The Zhaheba ophiolite consists of various igneous and metamorphic rock units. The igneous rocks include basalts, gabbros, and cumulates. The basalts are divided into Group I (alkaline) and Group II (subalkaline). The gabbros are mainly olivine gabbros and pyroxene gabbros. The cumulates include various types of pyroxenites and olivine pyroxenites. The metamorphic rocks include eclogites, omphacite pyroxenites, and amphibolites. The ages of the igneous rocks range from ~400 Ma to ~500 Ma. The ages of the metamorphic rocks range from ~400 Ma to ~500 Ma. The chemical composition of the basalts varies significantly, with Group I basalts being more alkalic than Group II basalts. The gabbros and cumulates show evidence of fractional crystallization, with increasing Fe/Mg ratios from olivine gabbros to pyroxene gabbros to pyroxenites. The metamorphic rocks show evidence of high-pressure metamorphism, with eclogites containing omphacite and pyroxene. The amphibolites contain plagioclase and amphibole. The overall geochemistry of the Zhaheba ophiolite is similar to other ophiolites in the region, such as the Dabie-Sulu Ophiolite and the Qinling-Dabie Ophiolite.



5.c. Petrogenesis of the Devonian basalts



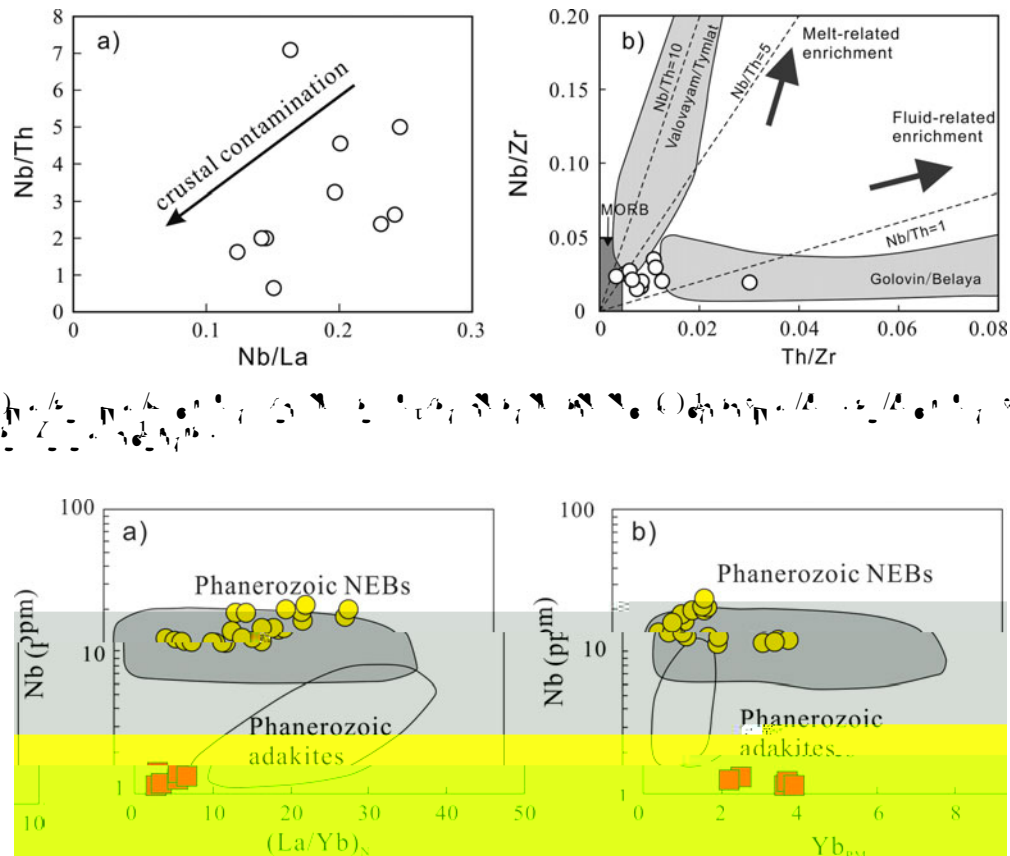


Fig. 12. (a) Nb/Th vs Nb/La; (b) Nb/Zr vs Th/Zr. Data are plotted according to the models of mantle melting and differentiation (MORB, Valovayam/Tymat, Nb/Th = 10, Nb/ThS, Nb/Th = 1, Golovin/Belya).

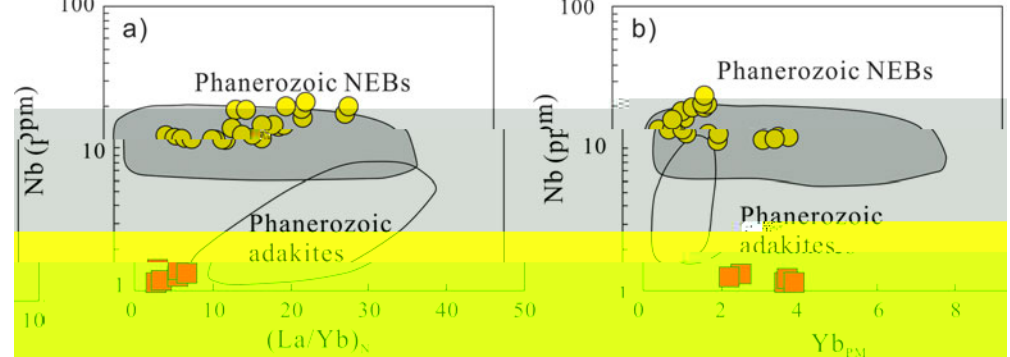
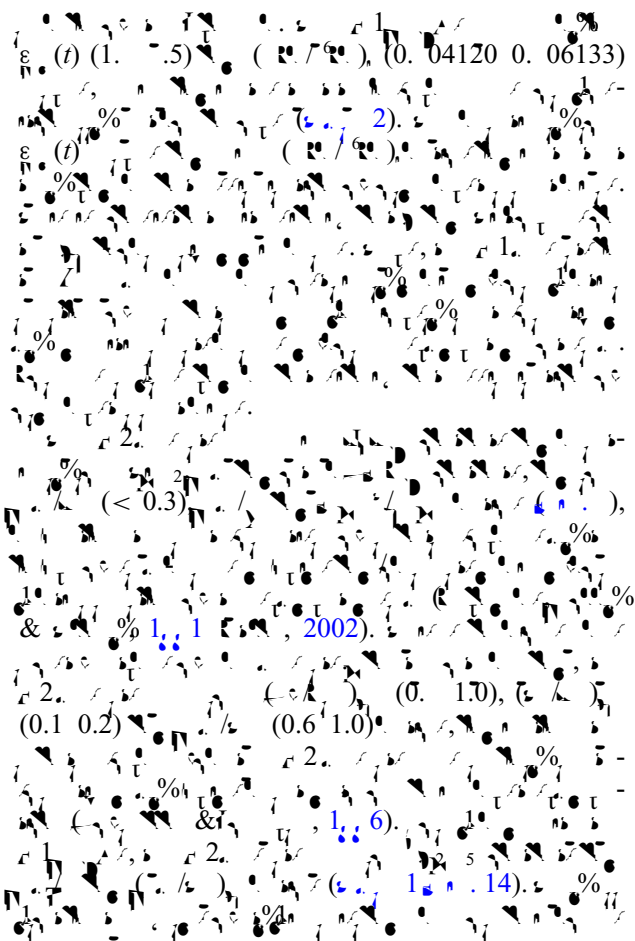
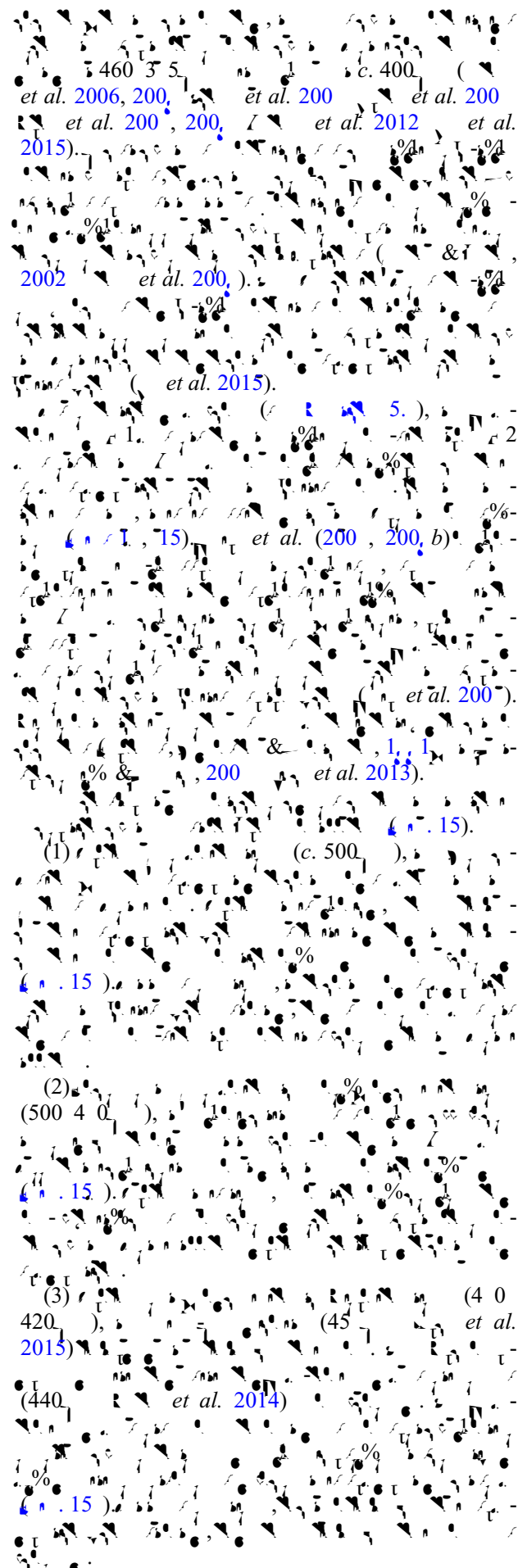
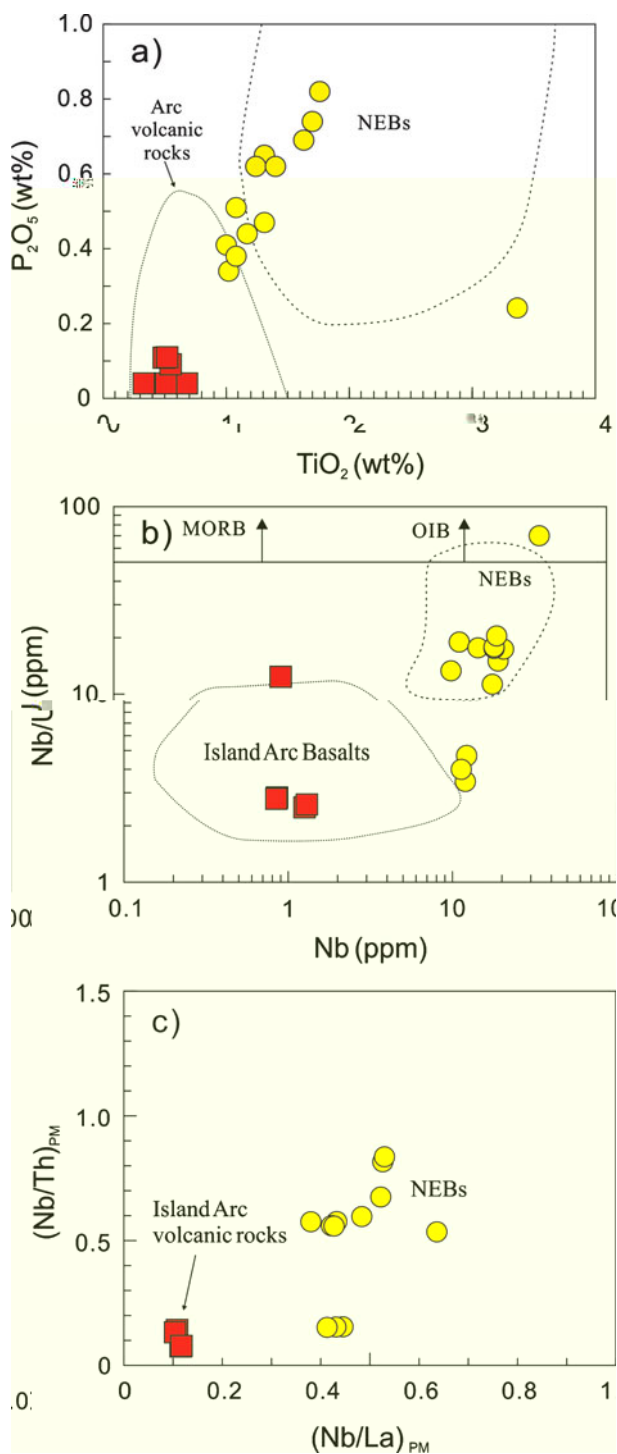


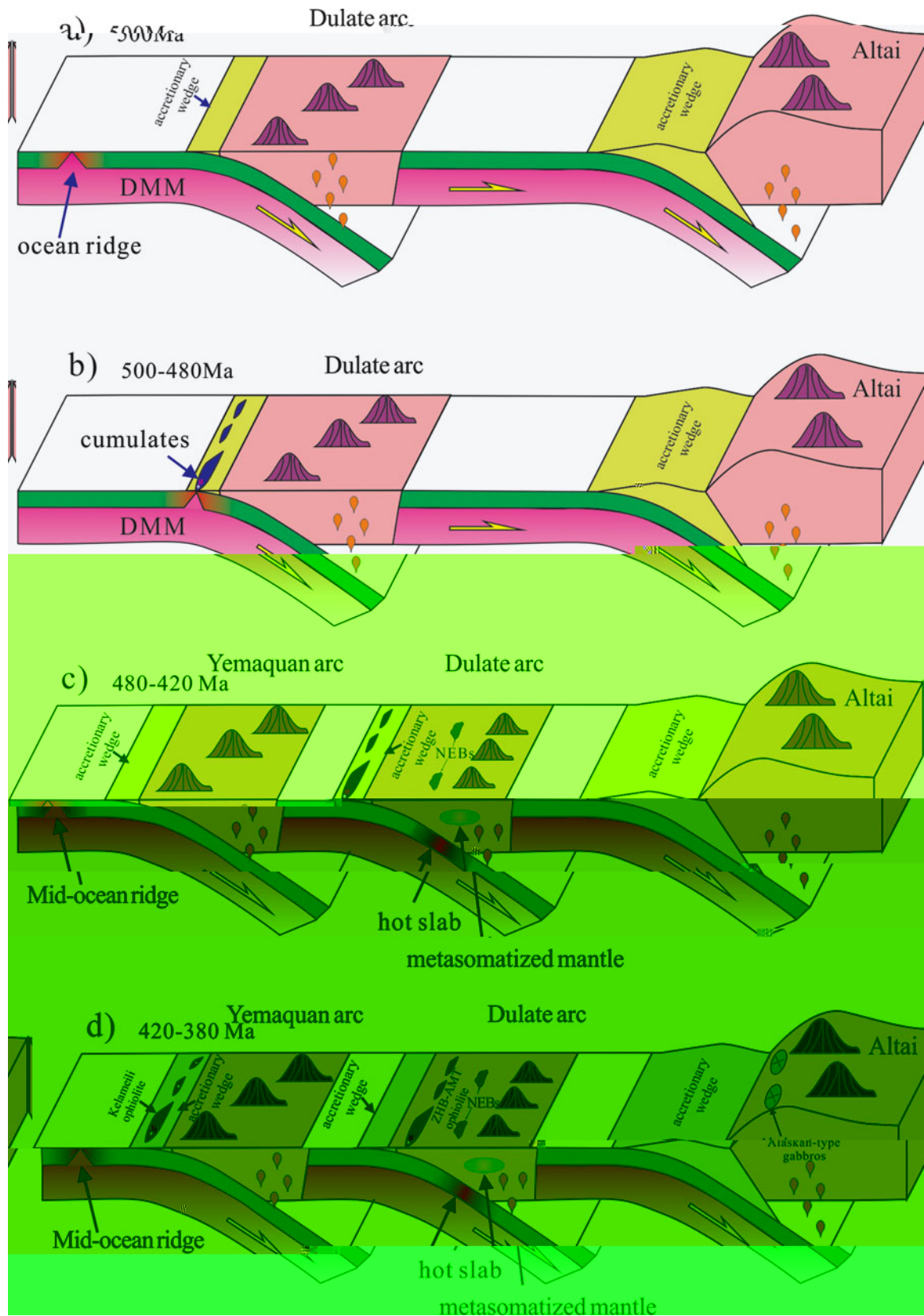
Fig. 13. (a) Nb vs (La/Yb)_N; (b) Nb vs Yb_{PM}. Data are plotted according to the Phanerozoic NEBs and adakites.

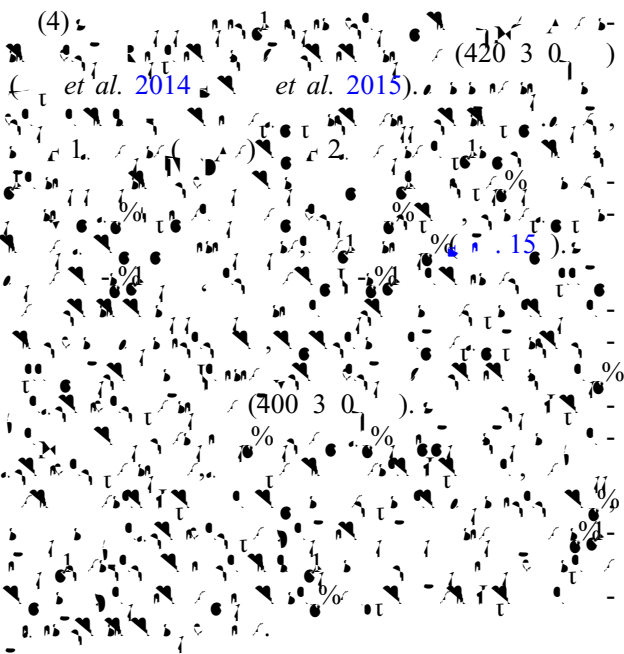


5. Implications for the Palaeozoic accretion process in eastern Junggar

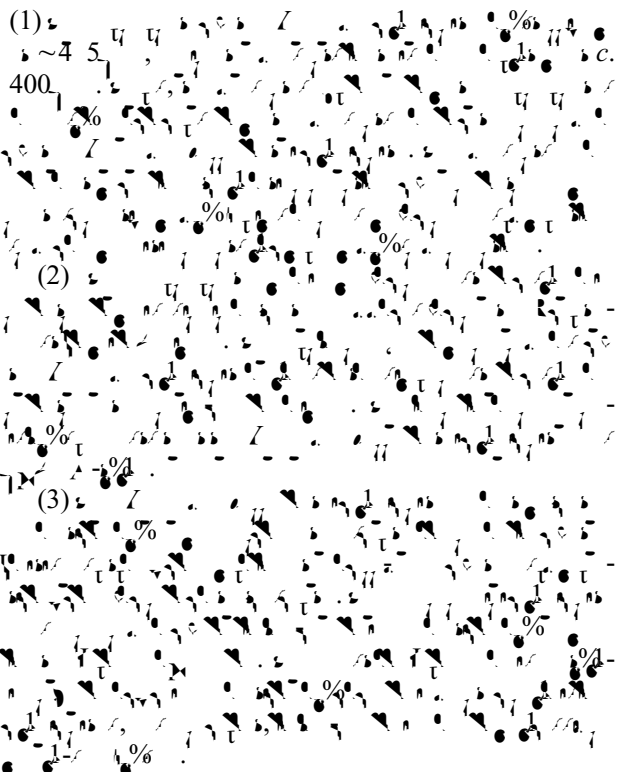
The Palaeozoic accretionary process in eastern Junggar is characterized by the formation of NEBs and adakites. The presence of NEBs suggests that the accretionary process involved the incorporation of older crustal material into the magmatic system. The presence of adakites suggests that the accretionary process involved the melting of older crustal material, likely due to the high temperatures associated with the accretion process. The presence of both NEBs and adakites suggests that the accretionary process was complex, involving both the incorporation of older crustal material and the melting of older crustal material. The presence of both NEBs and adakites suggests that the accretionary process was complex, involving both the incorporation of older crustal material and the melting of older crustal material.







6. Conclusions



Acknowledgments.

The authors would like to thank the anonymous reviewers for their useful comments and suggestions, which greatly improved the manuscript. This work was financially supported by the National Natural Science Foundation of China (41472225), the Chinese Ministry of Education (20140101120006), and the Chinese Academy of Geological Sciences (201401011200042). We also thank Dr. Liangzhen Li for his help with the ICP-MS analysis.

Supplementary material

<https://doi.org/10.1017/geo.2016.56> 16000042.

References

- (1) *et al. 2014* *et al. 2015*.
- (2)
- (3)
- (4)
- 1, 4. *et al. 2014* *et al. 2015*.
- Chemical Geology 113, 1, 1–204.
- &. 2001.
- Journal of Petrology 42, 22, 302.
- , 2000.
- Lithos 97, 2, 1.
- &. 2002.
- Geology 30, 0, 10.
- &. 2000.
- Earth Accretionary Systems in Space and Time (, &), 11, 1–36.
- &. 2002.
- Geological Magazine 139, 1, 13.
- , 2001.
- Geological Society of America Bulletin 105, 153.
- Ophiolites, 220, 11.
- &. 2001.
- Geology 21, 54–50.
- &. 2002.
- Journal of Geological Society, London 149, 56.
- &. 2003.
- Contributions to Mineralogy and Petrology 86, 54–6.
- &. 2003.
- (2) Ophiolites in Earth History (, &), 11, 43–6.
- 21.
- &. 2011.
- Geological Society of America Bulletin 123, 3, 411.
- , 2015.
- Chinese Journal of Geology 50, 140–54.
- &. 2000.
- Contributions to Mineralogy and Petrology 140, 23, 5.
- &. 2001.
- Lithos 27, 25.

- Liu, J., Li, Y., Lai, C., & Li, X. 2011. A new model for the formation of the South China Sea margin. *Geological Bulletin of China* 30, 150–153.
- Li, Y., Liu, J., & Li, X. 2011. The formation of the South China Sea margin. *Geochimica et Cosmochimica Acta* 75, 504–521.
- Li, Y., Liu, J., & Li, X. 2001. The formation of the South China Sea margin. *Nature* 410, 6–11.
- Li, Y., Liu, J., & Li, X. 2002. The formation of the South China Sea margin. *Chemical Geology* 182, 22–35.
- Li, Y., Liu, J., & Li, X. 2003. The formation of the South China Sea margin. *Journal of Geophysical Research: Solid Earth* (1978–2012) 101, 11–31.
- Li, Y., Liu, J., & Li, X. 2000. The formation of the South China Sea margin. *Contributions to Mineralogy and Petrology* 139, 20–26.
- Li, Y., Liu, J., & Li, X. 2012. The formation of the South China Sea margin. *Geological Bulletin of China* 31, 126–133.
- Li, Y., Liu, J., & Li, X. 2014. The formation of the South China Sea margin. *Chinese Science Bulletin (Chinese Version)* 59, 2213–2220.
- Li, Y., Liu, J., & Li, X. 2000. The formation of the South China Sea margin. *Transactions of the Royal Society of Edinburgh: Earth Sciences* 91, 1–13.
- Li, Y., Liu, J., & Li, X. 2001. The formation of the South China Sea margin. *Journal of Petrology* 31, 6–11.
- Li, Y., Liu, J., & Li, X. 2003. The formation of the South China Sea margin. *Earth Science Frontier* 10, 43–56.
- Li, Y., Liu, J., & Li, X. 2001. The formation of the South China Sea margin. *Journal of Petrology* 42, 655–671.
- Li, Y., Liu, J., & Li, X. 2000. The formation of the South China Sea margin. *Nature* 380, 23–40.
- Li, Y., Liu, J., & Li, X. 2000. The formation of the South China Sea margin. *Tectonophysics* 326, 255–261.
- Li, Y., Liu, J., & Li, X. 2010a. The formation of the South China Sea margin. *Lithos* 114, 1–15.
- Li, Y., Liu, J., & Li, X. 2004. The formation of the South China Sea margin. *Geological Magazine* 141, 225–231.
- Li, Y., Liu, J., & Li, X. 2010b. The formation of the South China Sea margin. *Geostandards and Geoanalytical Research* 34, 11–34.
- Li, Y., Liu, J., & Li, X. 2013. The formation of the South China Sea margin. *Chinese Science Bulletin* 58, 464–474.
- Li, Y., Liu, J., & Li, X. 2000. The formation of the South China Sea margin. *Lithos* 113, 2–4.
- Li, Y., Liu, J., & Li, X. 2010. The formation of the South China Sea margin. *Chinese Science Bulletin* 55, 1535–1546.
- Li, Y., Liu, J., & Li, X. 2003. User's Manual for Isoplot 3.00: A Geochronological Toolkit for Microsoft Excel. 4, 3–11.
- Li, Y., Liu, J., & Li, X. 2015. The formation of the South China Sea margin. *Gondwana Research*, 1–6. [10.1016/j.gr.2015.04.004](https://doi.org/10.1016/j.gr.2015.04.004).
- Li, Y., Liu, J., & Li, X. 2015. The formation of the South China Sea margin. *American Journal of Science* 274, 32–355.
- Li, Y., Liu, J., & Li, X. 2015. The formation of the South China Sea margin. *Geology* 43, 51–54.
- Li, Y., Liu, J., & Li, X. 2015. Structure of Ophiolites and Dynamics of Oceanic Lithosphere. *Acta Petrologica Sinica* 31, 36–51.
- Li, Y., Liu, J., & Li, X. 2015. The formation of the South China Sea margin. *Journal of Petrology* 55, 104–124.
- Li, Y., Liu, J., & Li, X. 2000a. The formation of the South China Sea margin. *Acta Petrologica Sinica* 25, 7–16.
- Li, Y., Liu, J., & Li, X. 2000b. The formation of the South China Sea margin. *Acta Petrologica Sinica* 25, 14–24.
- Li, Y., Liu, J., & Li, X. 2000c. The formation of the South China Sea margin. *Acta Petrologica Sinica* 25, 25–36.
- Li, Y., Liu, J., & Li, X. 2000d. The formation of the South China Sea margin. *Acta Petrologica Sinica* 25, 37–48.
- Li, Y., Liu, J., & Li, X. 2000e. The formation of the South China Sea margin. *Acta Petrologica Sinica* 25, 49–60.
- Li, Y., Liu, J., & Li, X. 2002. The formation of the South China Sea margin. *Proceedings of the Ocean Drilling Program, Scientific Results*, vol. 176, 1–16.

- Wang, Y., & Li, J. 2000. *Chinese Science Bulletin* 45, 216–221.
- Wang, Y., & Li, J. 2010. *Lithos* 117, 1–20.
- Wang, Y., & Li, J. 2000. *Journal of Asian Earth Sciences* 30, 666–675.
- Wang, Y., & Li, J. 2000. *Lithos* 100, 14–44.
- Wang, Y., & Li, J. 2014. *Elements* 10, 101–111.
- Wang, Y., & Li, J. 2001. *Contribution to Mineralogy and Petrology* 141, 36–52.
- Wang, Y., & Li, J. 2013. *Gondwana Research* 24, 3–2411.
- Wang, Y., & Li, J. 2013. *Journal of Petrology* 53, 6–26.
- Wang, Y., & Li, J. 2013. *Precambrian Research* 231, 301–24.
- Wang, Y., & Li, J. 2012. *Precambrian Research* 192–195, 1–20.
- Wang, Y., & Li, J. 2012. *Philosophical Transactions of the Royal Society of London* 335, 3–2.
- Wang, Y., & Li, J. 2013. *Nature* 377, 5, 5–600.
- Wang, Y., & Li, J. 2013. *Nature* 364, 2, 30.
- Wang, Y., & Li, J. 2014. *Lithos* 206–207, 234–51.
- Wang, Y., & Li, J. 2002. *Reviews of Geophysics* 40, 3–1–3–3.
- Wang, Y., & Li, J. 2000. *Journal of Geological Society, London* 161, 33, 42.
- Wang, Y., & Li, J. 2000. *Science in China Series D – Earth Sciences* 52, 1345–55.
- Wang, Y., & Li, J. 2000. *Magmatism in the Ocean Basin* (Wang, Y. & Li, J., eds), 11–52, 42.
- Wang, Y., & Li, J. 2000. *Chemical Geology* 247, 352–353.
- Wang, Y., & Li, J. 2000. *Acta Petrologica Sinica* 23, 1, 33–44.
- Wang, Y., & Li, J. 2000. *Contributions to Mineralogy and Petrology* 133, 1–11.
- Wang, Y., & Li, J. 2006. *Journal of Geology* 114, 35–51.
- Wang, Y., & Li, J. 2000. *Lithos* 110, 35–2.
- Wang, Y., & Li, J. 2012. *Earth-Science Reviews* 113, 303–41.
- Wang, Y., & Li, J. 2000. *Chemical Geology* 20, 325–43.
- Wang, Y., & Li, J. 2002. *Journal of Geology* 110, 1–3.
- Wang, Y., & Li, J. 2006. *Geology in China* 33, 4, 6–60.
- Wang, Y., & Li, J. 2014. *Geoscience Frontiers* 5, 525–36.
- Wang, Y., & Li, J. 2000. *Journal of Asian Earth Sciences* 32, 102–1.
- Wang, Y., & Li, J. 2013. *Gondwana Research* 23, 1316–41.
- Wang, Y., & Li, J. 2004. *Journal of Geological Society, London* 161, 33, 42.

- Wang, J., Li, H., Wang, Y., et al. 2000. *a.* Regional geological setting of the Zhaheba ophiolite, Xinjiang, China. *International Journal of Earth Sciences* **98**, 11–21.
- Wang, J., Li, H., Wang, Y., et al. 2000. *b.* Tectonic evolution of the Zhaheba ophiolite, Xinjiang, China. *American Journal of Sciences* **309**, 221–240.
- Wang, J., Li, H., 1993. Regional Geology of the Xinjiang Uygur Autonomous Region. *Geological Survey of China*, 11, 2, 145 pp.
- Wang, J., Li, H., 2015. Tectonic evolution of the Zhaheba ophiolite, Xinjiang, China. *Journal of Asian Earth Sciences* **113**, 5–15.
- Wang, J., Li, H., 2012. Tectonic evolution of the Zhaheba ophiolite, Xinjiang, China. *Gondwana Research* **21**, 246–265.
- Wang, J., Li, H., & Wang, Y., 2000. *c.* Tectonic evolution of the Zhaheba ophiolite, Xinjiang, China. *Chemical Geology* **242**, 223–246.
- Wang, J., Li, H., Wang, Y., et al. 2006. Tectonic evolution of the Zhaheba ophiolite, Xinjiang, China. *Acta Geologica Sinica* **80**, 254–263.
- Liu, X., Li, H., Wang, J., et al. 2003. Tectonic evolution of the Zhaheba ophiolite, Xinjiang, China. *Chinese Science Bulletin* **48**, 2231–2235.
- Liu, X., Li, H., Wang, J., et al. 2013. Tectonic evolution of the Zhaheba ophiolite, Xinjiang, China. *Lithos* **179**, 263–274.
- Liu, X., Li, H., Wang, J., et al. 2012. Tectonic evolution of the Zhaheba ophiolite, Xinjiang, China. *Journal of Asian Earth Sciences* **52**, 11–33.
- Liu, X., Li, H., Wang, J., et al. 2000. Tectonic evolution of the Zhaheba ophiolite, Xinjiang, China. *Acta Petrologica Sinica* **24**, 1054–1065.
- Hacker, B.R., & Van Heege, R.A., 1996. Tectonic evolution of the Zhaheba ophiolite, Xinjiang, China. *Annual Review of Earth and Planetary Sciences* **14**, 43–51.